AAS 95–314

Mars Gravity Field from Satellite-to-Satellite Doppler Data*

A. Vijayaraghavan†
Jet Propulsion Laboratory
California Institute of technology
4800 Oak Grove Drive
Pasadena, California 91109.

An accurate description of the Martian gravity field is essential to support such activities as autonomous navigation and Mars landing during future missions. From covariance analysis for some specific ewes, satellite-to-satellite (STS) Doppler data is known to be useful in accurately determining the gravitational field. In this paper, an approximate analysis is presented to show that the knowledge of the Mars gravity field can be improved by a factor of 10 to 20 with STS Doppler data. Both high-low and low-low satellite configurations are examined. The analysis is in the frequency domain proceeding from two-dimensional Fourier transforms of Hill's variational equations. 'I'he transfer functions for high-low and low-low STS data are obtained and an optimal filter is derived. The results are applicable for the determination of short wavelength gravitational field.

INTRODUCTION

The Mars Global Surveyor and the Mars Pathfinder spacecraft are scheduled to be launched by the end of 1996. NASA is giving serious consideration to a Mars Surveyor program with two launches at every opportunity through the year 2005. la this context, two or more satellites are likely to orbit Mars simultaneously during some overlapping period of their lifetime. It has been shown[1] by detailed covariance analysis (of a few cases) that satellite-to-satellite (STS) Doppler data is very useful in the accurate determination of the Martian gravity field. In this paper, an approximate analysis is presented for a preliminary assessment on the improvement to be obtained in the high-frequency or short wavelength Martian gravity field with STS Doppler data, avoiding costly, time-consuming and computation-intensive covariance analysis. With the present emphasis on on-board and autonomous navigation, STS Doppler data may become a reality in the not so distant future.

Satellite-to-satellite Doppler data can be obtained in two different configurations of the two spacecraft involved. (In this paper, sometimes Satellite-to-satellite Doppler data will also be designated as STS data, for convenience.) A Communications-Relay cum Navigation Satellite may be deployed in a high orbit (of radius possibly 15,000-30,000 km) about Mars and the other in a low orbit at an altitude of about 200 km. This case will be referred to as the high-low satellite configuration.

† Member, '1'ethnical Staff, Navigation and Flight Mechanics Section

* This work was carried out at the Jet Propulsion Laboratory, California Institute of Technology, Pasadena, California under contract to the National Aeronautics and Space Administration.

Otherwise, two spacecrafts in low orbits such as for high-resolution imaging purposes or atmospheric studies, may be considered for STS data. The latter will be designated as the low-low satellite configuration. Both these cases are examined in the analysis below and the detailed results will be presented in the paper.

Some Preliminaries

The analysis is based on Hill's variational equations for circular orbits. The perturbations are considered to be derived from gravitational harmonics only. In particular, the probelm is solved using two-dimensional Fourier transforms in Cartesian coordinates (for the upper half-space) for the conservative gravitational field. Due to the assumptions made in the analysis, the results must be considered appropriate for high-frequency or short wavelength harmonics only.

The STS data consists of the relative velocity between the two satellites under consideration. For satellites in the high-low configuration, the satellite in high orbit is essentially unaffected by the higher degree and order gravitational harmonics except the fundamental, spherically symmetric field. Hence the relative velocity between the spacecraft can be attributed to the high frequency gravitational field only. In the low-low configuration, for two satellites in the same low circular orbit, but separated by a finite distance (separated in true anomaly) between them, the relative velocity is obtained from the change in the non-spherical gravitational field due to the difference between the spacecraft positions.

The relative velocity between the two spacecraft is derived in the (Fourier) transform domain in terms of the high-frequency (or non-spherical) part of the gravitational field by solving Hill's equations. The down-track, cross-track and radial (positive outward) directions of the rotating coordinate system attached to the spacecraft will be identified with the positive x, y and z directions of the upper half-space. In turn, the Cartesian coordinates of the upper half-space will lead to solving the problem in the frequency domain by Fourier transforms. The perturbation forces in Hill's equations are also expressed in terms of the two-dimensional Fourier transforms of the anomalous (or spherically asymmetric part of the) gravitational field for these purposes. With an optimal filter in the frequency domain, the improvement in the spatial power spectral density of the gravity field is evaluated from the relative velocity measurements or STS (Doppler) data. This procedure primarily completes the analysis.

All the results from the crucial steps of the analysis are included in this paper for both the high-low and low-low satellite configurations. Results of parametric studies varying the satellite altitude and data noise are presented and discussed.

ANALYSIS

Hill's equations[2] for he perturbations of a spacecraft nominally n a circular orbit are given by

$$\ddot{\xi} - 2n\dot{\eta} - 3n^2\xi = f_\xi \tag{1}$$

$$\ddot{\eta} + 2n\dot{\xi} = f_\eta \tag{2}$$

$$\ddot{\zeta} + n^2\zeta = f_\zeta \tag{3}$$

where (ξ, η, ζ) arc the perturbations in the spacecraft position in tile radial, down-track and cross-track directions respectively. $\dot{\xi}$ and $\ddot{\xi}$ denote the velocity and acceleration in the radial direction and similarly $(\dot{\eta}, \ddot{\eta})$ and $(\zeta, \ddot{\zeta})$ in the down-track and cross-track directions. n denotes the mean motion of the spacecraft in its nominal circular orbit and $(n = V_0/R)$, where V_0 and R arc the nominal circular speed and orbital radius.

The most crucial assumption in the approximate analysis is that the planetary surface shall be considered "flat". In particular, let the Cartesian $(x\text{-}y)$ plane denote the planetary surface with the x axis parallel to the nominal down-track motion of the spacecraft and the y axis parallel to the cross-track direction and pointing in the same manner. The z axis points 'radially upward", in the upper half-space.

With this nomenclature, it is readily seen that

$$\dot{\xi} = (d\xi/dx)(dx/dt) = V_0 (d\xi/dx) \tag{4}$$

and similarly, $\ddot{\xi} = -V_0^2 (d^2\xi/dx^2)$. In turn, the perturbation Eqs. (l-3) can be rewritten as in

$$V_0^2 \xi'' - 2nV_0\eta' - 3n^2\xi = f_\xi \tag{5}$$

$$V_0^2 \eta'' + 2nV_0\xi' = f_\eta \tag{6}$$

$$V_0^2 \zeta'' + n^2\zeta = f_\zeta \tag{7}$$

where (') and (") denote the first and second derivatives with respect to x. The two-dimensional Fourier transforms in (x, y) of Eqs. (5), (6) and (7) are readily obtained:

$$-(\omega_x^2 V_0^2 + 3n^2)\tilde{\xi} - 2nV_0 j\omega_x\tilde{\eta} = \tilde{f}_\xi \tag{8}$$

$$2nV_0 j\omega_x \tilde{\xi} - \omega_x^2 V_0^2 \tilde{\eta} = \tilde{f}_\eta \tag{9}$$

$$-\omega_x^2 V_0^2 \tilde{\zeta} + n^2 \tilde{\zeta} = \tilde{f}_\zeta \tag{lo}$$

where the Fourier transform of any function G(x, y; z) has been implicitly defined as in

$$\tilde{G}(\omega_x, \omega_y; z) = \int\int G(x, y; z) \exp\{-j(\omega_x x + \omega_y y)\}\, dx\, dy. \tag{11}$$

The perturbation forces (f_ξ, f_η, f_ζ) and their transforms are derived from the scalar anomalous gravitational potential $G(x, y; z)$ and its transform, $\tilde{G}(\omega_x, \omega_y; z)$. In particular, $G(x, y; z)$ satisfies Laplaces's equation, with prescribed values on the surface, z = O;

$$V^2 G = O; \quad G(x, y; 0) = G(x, y). \tag{12}$$

It is easily derived[3,4] that

$$\tilde{G}(\omega_x, \omega_y; z) = G(w)\, e^{-|\omega| z}, \quad (W^2 = \omega_x^2 + \omega_y^2) \tag{13}$$

where $G(\omega)$ and $G(x, y, ; O)$ are Fourier transform pairs. Since the perturbation forces are obtained from the (negative of the) gradient of the anomalous gravitational potential,

$$(f_\xi, f_\eta, f_\zeta) = -(\partial/\partial z, \partial/\partial x, \partial/\partial y) G(x, y; z) \tag{14}$$

$$(\tilde{f}_\xi, \tilde{f}_\eta, \tilde{f}_\zeta) = (|\omega|, -j\omega_x, -j\omega_y)\, \tilde{G}(\omega) e^{-|\omega| z}. \tag{15}$$

Substituting Eq. (15) in Eqs. (8) through (1 O), solutions for the perturbations in the spacecraft position arc obtained in the transform domain as follows:

$$\tilde{\xi} = -\{|\omega|/(\omega_x^2 V_0^2)\}\, \tilde{G}(\omega)\, e^{-|\omega|h} \tag{16}$$

$$\tilde{\eta} = \{j\omega_x/(\omega_x^2 V_0^2)\}\, \tilde{G}(\omega)\, e^{-|\omega|h} \tag{17}$$

$$\tilde{\zeta} = \{j\omega_y/(\omega_x^2 V_0^2)\}\, \tilde{G}(\omega)\, e^{-|\omega|h} \tag{18}$$

where, the spacecraft nominal altitude, '$z = \mathbf{h}$', above the planetary surface has specifically been entered in the equations and it has also been assumed that $R\omega_x \gg 1$.

Since the relative velocity in the down-track direction, $v_x = (d\eta/dt) = V_O\,(d\eta/dx)$, its transform is given by (from the definition in Eq. (11) and Eq. (17) for $\tilde{\eta}$)

$$\tilde{v}_x = (j\omega_x)V_0\tilde{\eta} = -(1/V_0)\tilde{G}(\omega)e^{-|\omega|h}. \tag{19}$$

Similarly, it is easily shown that

$$\tilde{v}_y = (j\omega_x)V_0\tilde{\zeta} = -(\omega_y/\omega_x)(1/V_0)\tilde{G}(\omega)\, e^{-|\omega|h} \tag{20}$$

$$\tilde{v}_z = (j\omega_x)V_0\tilde{\xi} = (|\omega|/j\omega_x)\,(1/V_0)\tilde{G}(\omega)\, e^{-|\omega|h}. \tag{21}$$

Eqs. (19), *(20)* and (21) arc the **measurement equations** of the Doppler data on the relative velocity between two satellites in the high-low configuration.

The relative velocity v_{ll}, between 2 satellites separated by a distance A in the same low circular orbit (low-low configuration) is given by[5]

$$v_{ll} = v_x(x + \mathrm{A}/2) - v_x(x - \mathrm{A}/2)$$

$$= \Delta \frac{d}{dx}\left\{ V_0 \frac{d\eta}{dx}\right\} = V_0\, \Delta \frac{d^2\eta}{dx^2}$$

so that in the transform domain

$$\tilde{v}_{ll} = -(2/V_0)j \sin(\omega_x\Delta/2)\, \tilde{G}(\omega)\, e^{-|\omega|h} \tag{22}$$

In this paper, the *gaussian-weighted average of the pointwise or* local *surface gravity anomaly* is examined for evaluating the merits of determining the high-frequency gravity field with satellite-to-satellite Doppler data. Let $\lambda(x, y)$ and $\lambda_{av}(x, \mathrm{y})$ denote the pointwise surface gravity anomaly and its gau ssian-weight cd average; they are given by

$$\lambda(x, \mathrm{y}) = -(\partial/\partial z)\, G(x, y; z) \text{ at } z = \mathrm{O} \tag{23}$$

$$\lambda_{av}(x,\ Y) = \frac{1}{2\pi\sigma^2} \iint \lambda(p, q)\, \exp\{-\frac{1}{2\sigma^2}[(x - p)^2 + (y - q)^2]\}\, dp\, dq \tag{24}$$

where σ is the appropriately chosen[4] 'spread' of the gaussian weighting kernel. It may be noted that the 'pointwise surface gravity anomaly' is simply the radial or z-directional acceleration f_ξ on the planetary surface (at z = O) as in Eqn. (14).

Let $\hat{\lambda}_{av}(x, y)$ be the **"optimally estimated"** gaussian-averaged pointwise surface gravity anomaly and $\bar{\lambda}_{av}$ denote the error as in

$$\bar{\lambda}_{av}(x, y) = \hat{\lambda}_{av}(x, y) - \lambda_{av}(x, y) \tag{25}$$

Then the merits of determining the high-frequency gravity field with data from satellites in the "high-low" and "low-low" configuration will be evaluated by the minimum value(s) of the square-error integral in the estimated surface gravity anomaly (gaussian-averaged) as in

$$\lambda^* = \text{Min E}\{[\bar{\lambda}_{av}(x, y)]^2\} \tag{26}$$

$$= \iint \{\hat{\lambda}_{av}(x, y) - \lambda_{av}(x, y)\}^2 \, dx \, dy \tag{27}$$

By definition (and choice) the **optimal estimator** will yield the minimum square-error integral in equations (26) and (27). In particular, it follows from Parseval's theorem that

$$\lambda^* = (1/4\pi^2) \iint \|\bar{\lambda}_{av}\|^2 \, d\omega_x \, d\omega_y \tag{28}$$

$$= (1/4\pi^2) \iint \{\hat{\lambda}_{av}(\omega) - \lambda_{a\ v}(\omega)\}^2 d\omega_x d\omega_y. \tag{29}$$

From now onwards, the (ˆ) above the argument as in $\hat{\lambda}(\omega)$, denoting Fourier transform will be dropped for convenience; the context will make it clear, when the discussion is in the frequency (ω) domain.

Furthermore, from equations (13), (15), (23) and (2.5), $\lambda(\omega)$ and $\lambda_{av}(\omega)$ can be obtained as in

$$\lambda(\omega) = |\omega| \, G(\omega) \tag{30}$$

$$\lambda_{av}(\omega) = |\omega| \exp(-\sigma^2\omega^2/2) \, G(\omega) \tag{31}$$

$$= p(\omega) \, G(\omega) \tag{32}$$

$$\text{where } p(\omega) = |\omega| \exp(-\sigma^2\omega^2/2) \tag{33}$$

Let the general k-vector of measurements be denoted by

$$d(\omega) = H(\omega) \, G(\omega) + W \tag{34}$$

$d(\omega)$ is the S'1'S Doppler (observational) data. $H(\omega)$ is the transfer function between the observations and the anomalous gravitational field $G(\omega)$, as in equations (19)-(21) for two satellites in the high-low configuration and as in (22) for low-low satellites. W is a k-vector of measurement (noise) errors. Let $\hat{\lambda}_{av}(\omega)$ be optimally determined from

$$\hat{\lambda}_{av}(\omega) = \psi^T(\omega) \, d(\omega) = \psi^T(\omega) \, [H(\omega) \, G(\omega) + W] \tag{35}$$

where $\psi(\omega)$ is a k-vector optimal estimator and the superscript $()^T$, implies the transpose in matrix algebra. From (32) and (35), it is readily seen that

$$\bar{\lambda}_{av}(\omega) = \{\psi^T(\omega) \, H(\omega) - p(\omega)\} \, G(\omega) + \psi^T(\omega) \ W \tag{36}$$

$$\|\bar{\lambda}_{av}(\omega)\|^2 = \{\psi^T(-j\omega) \, H(-j\omega) - p(-j\omega)\} \, \Phi_G(\omega) \, \{H^T(j\omega) \, \psi(j\omega) - p(j\omega)\} + \psi^T(-j\omega) \, \Phi_W(\omega) \, \psi(j\omega) \tag{37}$$

$$\text{where } \Phi_G(\omega) = \text{E}\{\|G(\omega)\|^2\}. \tag{38}$$

Similarly, @w(~) is the power spectral density of the measurement noise. Since the integrand in (28) is positive semi-definite, the minimum value of the integral for λ^* is attained, if the filter $\psi(\omega)$

is chosen so that the first variation $\delta \|\bar{\lambda}_{av}(\omega)\|^2 = 0$. In fact, from Eq. (37), the first variation is derived as in

$$\delta \|\bar{\lambda}_{av}(\omega)\|^2 = \delta\psi^T(-j\omega)\{H(-j\omega)\,\Phi_G(\omega)\,[H^T(j\omega)\,\psi(j\omega) - p(j\omega)] + \Phi_W(j\omega)\,\psi(j\omega)\} + \{[\psi^T(-j\omega)\,H(-j\omega) - p(j\omega)]\,\Phi_G(\omega)\,H^T(j\omega) + \psi^T(-j\omega)\,\Phi_W(\omega)\}\,\delta\psi(j\omega). \tag{39}$$

The condition that the first variation must vanish for any arbitrary choice of $\delta\psi$, implies that the terms within the curly brackets in Eq. (39) must equal O. Hence the optimal filter is given by

$$\psi(\omega) = \{H(-j\omega)\,\Phi_G(\omega)\,H^T(j\omega) + \Phi_W(\omega)\}^{-1}\ If(-'jLA))\ \Phi_G(\omega)\,p(j\omega) \tag{40}$$

with necessary assumptions on data noise and the gravitational potential so that all cross-correlations vanish identically. Substituting Eq. (40) in (37) and using "the matrix-inversion lemma"

$$\{A_1 - A_{12}\,A_2^{-1}\,A_{21}\}^{-1} = A_1^{-1} + A_1^{-1}\,A_{12}\,\{A_2 - A_{21}\,A_1^{-1}\,A_{12}\}^{-1}\,A_{21}\,A_1^{-1}$$

with $A1 = \Phi_W$, $A_2^{-1} = \Phi_G$, $A_{12} = H$ and $A_{21} = H^T$, it is readily seen that the integrand in Eq. (28) can be rewritten as in

$$\|\bar{\lambda}_{av}(\omega)\|^2 = \frac{\Phi_G(\omega)\,p(-j\omega)\,p(j\omega)}{1 + \Phi_G(\omega)\,H^T(j\omega)\,\Phi_W^{-1}\,H(-j\omega)}. \tag{41}$$

In particular, for the optimal estimator, the minimum square-error integral λ^* (the familiar 'cost function") is given by

$$\lambda^* = \text{Min}\ E\{\|\bar{\lambda}_{av}(\omega)\|^2\} = \frac{1}{4\pi^2}\iint \frac{\Phi_G(\omega)\,p(-j\omega)\,p(j\omega)}{1 + \Phi_G(\omega)\,H^T(j\omega)\,\Phi_W^{-1}\,H(-j\omega)}\,d\omega_x\,d\omega_y. \tag{42}$$

High-Low Satellite-to-Satellite Doppler Measurements

For the high-low satellites, from Eqs. (19)-(21), the transfer function can be written as in

$$H_{hl}(\omega) = -\exp(-\omega h)\,(1/V_0)\,\{1,\ (\omega_y/\omega_x),\ -j(w/wZ)\}. \tag{43}$$

Substituting Eq. (43) in (42) and transforming to polar coordinates in the $(\omega_x - \omega_y)$ plane, we obtain

$$\lambda_{hl}^* = \frac{1}{2\pi}\int_0^\infty p^2(\omega)\,\Phi_G(\omega)\left[\frac{1}{2\pi}\int_0^{2\pi}\frac{d\alpha}{1 + 2\,A_{hl}(\omega)\sec^2\alpha}\right]\omega\,d\omega \tag{44}$$

where $A_{hl}(\omega) = \Phi_G(\omega)\,exp(-2\,\omega\,h)\,(1/V_0^2)\,\{N/\ (2\pi^2 R^2 \sigma_m^2)\}$. (45)

N is the total number of Inca.surements, σ_m the high-low STS data noise and R is the planetary radius in Eq. (45). In particular, the last term in the curly brackets denotes the "uniform" density of measurements per unit area, with the Mercator projection area for Mars being used, to make the measurement density independent of latitude. The inner integral within the square brackets

in Eq. *(44)* has all the information from observations. The reduction in the variance (from the *a priori)* given by the inner integral is easily calculated from

$$D_{hl}^2 = \frac{1}{2\pi}\int_0^{2\pi} \frac{d\alpha}{1 + 2\,A_{hl}(\omega)\,\sec^2\alpha}$$
$$= 1 - \{2\,A_{hl}(\omega)\}^{1/2}\{1 + 2\,A_{hl}(\omega)\}^{-1/2} \qquad (46)$$

for each spatial frequency, w. The notation D_{hl}^2 in Eq. (46), stands for the reduction of the power spectral density of the error in average surface gravity anomaly, due to the information obtained from the high-low satellite-to- satellite Doppler data. D_{hl} (w) is itself a measure of the effectiveness of the data at any given frequency, w. The frequency response, $D_{hl}(\omega)$ will be shown plotted for various cases when discussing results.

The "outer integral" in Eq. (44) for the square error integral in the average surface gravity anomaly, can be obtained by numerical integration of

$$\lambda_{hl}^* = \frac{1}{2\pi}\int_0^{\infty} p^2(\omega)\,\Phi_G(\omega)\,D_{hl}^2(\omega)\,w\,d\omega \qquad (47)$$

where p(w) = w exp$(-\sigma_{av}^2\omega^2/2)$ for the average surface gravity anomaly. σ_{av} denotes the "averaging distance", for the Gaussian kernel over the planetary surface, taken to be about 59.29 km for Mars corresponding to 10. The *a priori* average gravity anomaly and the a *posterior* error in the average gravity anomaly (the radial acceleration on the surface and the residual error) are presented in the Table at the end.

Low-Low STS **Data Measurements**

For two satellites in the low-low configuration, from Eq. (32) the transfer function is given by

$$H_{ll}(\omega) = -(2j)\exp(-\omega h)(1/V_0)\sin(\omega_x\Delta/2) \qquad (48)$$

where A is the **separation distance between the satellites.** From Eqs. (48) and (42), it is **easily derived**

$$\lambda_{ll}^* = \frac{1}{2\pi}\int_0^{\infty} p^2(\omega)\,\Phi_G(\omega)\left[\frac{1}{2\pi}\int_0^{2\pi}\frac{d\alpha}{1 + A_{ll}(\omega)\cos^2\alpha}\right]\omega\,d\omega \qquad (49)$$

$$\text{where}\quad A_{ll}(\omega) = \Phi_G(\omega)\,exp(-2\omega h)(1/V_0^2)\,\omega^2\,A'\,\{N/(2\pi^2R^2\sigma_m^2)\}. \qquad (50)$$

The dependency on the separation distance A is clearly brought out in Eq. (50); once again, σ_m stands for measurement noise.

The reduction in the degree variance for the low-low satellite system is given by

$$D_{ll}^2 = \frac{1}{2\pi}\int_0^{2\pi}\frac{d\alpha}{1 + A_{ll}(\omega)\cos^2\alpha}$$
$$= \frac{1}{\sqrt{1 + A_{ll}(\omega)}} \quad \text{at each spatial frequency, } \omega. \qquad (51)$$

In the case of the low-low satellite observation system, the effects of planetary rotation on the transfer function and on the results in Eqs. (49) and (51) are significant Since a rotation in the $x-y$ plane corresponds to a rotation of equal magnitude in the Fourier transforms, Eq. (49) just gets modified as in

$$\lambda_{ll}^{*} = \frac{1}{2\pi}\int_0^{\infty} p^2(\omega)\,\Phi_G(\omega)\left[\frac{1}{2\pi}\int_0^{2\pi}\frac{d\alpha}{1+\frac{1}{2}\,A_{ll}(\omega)\left[\cos^2(\alpha-\delta)+\cos^2(\alpha+\delta)\right]}\right]\omega\,d\omega. \quad (52)$$

Analogous to Eq. (51), D_{ll}^2 is given by

$$D_{ll}^2 = \frac{1}{\sqrt{[1+A_{ll}(\omega)]\,[1+\delta^2\,A_{ll}(\omega)]}} \quad (53)$$

In Eqs. *(52)* and (53) above, δ denotes the angle by which Mars rotates about its axis during one period of the orbiting low-low satellite system. The planetary rotation dots not play any significant role in the high-low observations.

The frequency response of the low-low satellite system $D_{ll}(\omega)$ will be shown plotted for several cases in the section on results. Also, the *a priori* average surface gravity anomaly and *a posterior* error values for a number of low-low satellite-to-satellite observation systems are shown tabulated in the end. For the sake of brevity, only results including planetary rotation correction will be discussed for the low-low satellite systems.

Review of Analysis

Proceeding from Hill's equations, Doppler measurement of the relative velocity between two satellites is shown related to the anomalous gravitational potential as in Eqs. (19) through (22). Then a minimum cost criterion is stipulated as given in Eqs. (26) through (29) in terms of the estimation error in the averaged pointwise surface gravity anomaly, squared and integrated over the 'planetary surface'. The optimal estimator is derived in (40) and the minimum value of the square-error integral is obtained in (42) depending upon the data type (for the transfer function) and the power spectral density of the data noise and of the surface gravity anomaly. This completes the analysis.

RESULTS ANI) CONCLUSIONS

'he reduction in the estimation error in the average surface gravity anomaly, D_{hl}, corresponding to the square-root of Eq. (46), with observations from the high-low satellite system, is shown plotted in Figure 1. It is useful to recall that the **lower the reduction** factors are, the more desirable the observational system is for the determination of the Martian gravitational field,

The curves in Figure 1 provide information on the frequency response of the high-low satellite-to-satellite Doppler measurements. The number of obser vations is taken to be 25,000 at a Doppler noise level of 0.1 mm/s. Three different PSI) (power spectral density) profiles for the *a priori* anomaly, are examined. 'l'hey include the spectra of the gravitational potential coefficients and of the uncertainties in the coefficients (namely, "σ"s) published by Konopliv and Sjogren[7]. The third *a priori* 1'S1) for examination throughout this paper is given by Kaula's rule for Mars[8]:

$$\text{Degree Variance} = \sum_{m=0}^{n}(\bar{a}_{nm}^2+\bar{b}_{nm}^2) = (2n+1)\,\frac{1.69\times10^{-8}}{n^4} \quad (54)$$

The high-low S1'S data is seen to best advantage at the "low" to intermediate frequencies in the figure; it must be remarked that the analysis is based clearly on the assumption of high frequency perturbations both in terms of Fourier transforms as well as in the derivation of the relative velocity transfer functions for the observation systems. Since the "power" at low frequencies (corresponding to the harmonics of degree 2 through 10, say) is substantial, consistent with the role of the a *priori* as seen in Eqs. (45) and (46), highly sensitive response is indicated in Figure 1, which however, is not valid. On the contrary, since the PSD of the uncertainties is relatively very small at the low degree gravitational harmonics (which are well known), there is no substantial improvement to be obtained from high-low STS data corresponding to that frequency range as seen in Figure 1 from the response to the a *priori* from Mars50c-σs. At high spatial frequencies, the high-low system deteriorates in its response, though it is seen that upto degree and order 50, substantial improvement can be obtained in determining the Martian gravity field. *It must be remarked* that the high-low *STS* data analysis *here*, assumes that *all* the *three components of the relative velocity are fully* observable at each data *point, as if one were* to deal with a *GPS-like* system *of high* satellites.

Results of sensitivity studies (in terms of data noise and satellite altitude) are shown plotted in Figure 2. It is observed that when the Doppler noise level increases from 0.01 to 0.1 mm/s, the estimation error in the average surface gravity anomaly increases by about an order of magnitude for observations from high-low systems. Furthermore, at low (spatial) frequencies, while the altitude of the 'low' satellite of the high-low system is not too detrimental, it is seen that increasing the altitude from *200* to 378 km, reduces the "cut-off" spatial frequency corresponding to about 50 harmonics. At a reduction factor of 0.1, a satellite at 200 km altitude is superior to one at 378 km, at both measurement noise levels examined. In short, low altitudes are far more desirable.

The frequency response of low-low STS data observational systems is shown in Figures 3a and 3b. The general features of all the results discussed for the high-low configuration seem to be applicable for the case of low-low observational satellites also. A careful examination will reveal, in addition, that the low-low satellite response for the same data noise level and satellite(s) altitude is slightly inferior to that of the high-low system; however, changing the separation distance between the low-low satellites from 50 km (the nominal value in Figure 3) to higher values, alters this picture as will be seen in Figure 5.

A direct comparison of the high-low and low-low STS Doppler data observational systems is provided in Figure 4. At a separation distance of 50 km for the low-low satellites, (for the cases examined in Figure *4)* the low-low system seems to be inferior to the high-low system in terms of frequency response. Actually, the frequency response of the low-low system for a data noise level of 0.01 mm/s, falls clearly between the response curves for the high-low system corresponding to data noise levels of 0.01 and 0.1 mm/s. In Figure 5, the high-low satellite system is compared to the low-low system with a separation distance of 100 km (between the two low altitude satellites in the same circular orbit). At data noise levels of 0,001, 0.005 mm/s, the low-low system (with A = 100 km), is clearly superior in its frequency response characteristic, in comparison to a high-low system at 0.01 mm/s. At the same noise level of 0.01 nlm/see, the low-low system is just as good as the high-low examined here and in fact, is slightly better at high frequencies.

The results in Figure 6 are reproduced from Ref. (1), from detailed covariancc studies for a High-Low system. The high satellite was in an orbit at an inclination of about 10°, while the low satellite was in a polar orbit at about 380 km. The advantage of STS data in determining the Mars gravitational field is distinctly brought out from the *a posteriori* RMS spectrum. Actually, the *a priori* rms values for the gravity spectrum for harmonics of degree *20* and above, in those studies were approximately $2X\,10^{-7}$. The reduction achieved in the RMS spectra serves to confirm the

validity of the analysis presented" here.

Finally the square error integral in the average gravity anomaly, as given by Eqs. (47) and (52) (for the high-low and the low-low systems respectively) have been obtained by numerical integration. It may be noted that the *a priori* values are obtained, simply by integrating with the transfer functions set to zero. For the various cases examined, the results are shown in Table 1. The results arc very sensitive to the radius of the "averaging" Gaussian kernel. Both a 1° and (½°) spread have been considered. Results for separation distances of 50 and 100 km between the satellites arc presented for the low-low system. Once again, a low-low system with a separation distance of 100 km, seems to match the performance of the high-low system at the same data noise level.

ACKNOWLEDGEMENTS

It is a pleasure to thank W.E. Bellman, Supervisor, Maneuver Analysis Group and the management of the Navigation and Flight Mechanics Section, Jet Propulsion Laboratory, for all their encouragement in carrying out these studies and presenting this paper. W.L.Sjogren, Alex Konopliv and Stuart Demcak of the Jet Propulsion Laboratory have contributed significantly to the results here. W. Melbourne and Dave Sonnabend (formerly) of JPL brought this probelm to attention, and have participated in numerous discussions relating to this work. This work was carried out by the Jet Propulsion Laboratory, California Institute of Technology, Pasadena, under contract with the National Aeronautics and Space Administration.

REFERENCES

1. A. Vijayaraghavan et al., "Mars Gravity Field From Dual Satellite Observations," AAS 93-623, AAS/AIAA Astrodynarnics Specialist Conference, Victoria, B. C., Canada, August 16-19, 1993.

2. M. 11. .Kaplan, *Modern Spacecraft Dynamics and Control,* John Wiley & Sons., Inc., 1976.

3. A. Vijayaraghavan, "Frequency Domain Analysis for the Determination of Short Wavelength Gravity Variations," Engineering Memorandum EM 314-348, JPL Internal Document, October 1, 1984.

4. J. V. Breakwell, "Satellite Determination of Short Wavelength Gravity Variations," Journal of the Astronautical Sciences, Vol. XXVII, No. 4, October- December, 1979, pp. 329-344.

5. A. Vijayaraghavan, "On the relative velocity between two satellites in the same orbit," JPL IOM 314.4-662, JPL Internal Document, June 7, 1989.

6. A. Vijayaraghavan, "Frequency Domain Analysis for Mars Gravity Field Determination," JPL IOM 314.4-643, JP1, Internal Document, July 16, 1993.

7. A. S. Konopliv, W.L.Sjogren, *The JPL Mars* Gravity *Field Mars50c, Based* Upon Viking *and* Mariner 9 *Doppler Tracking* Data, JPI, Publication 95-5, February 95.

8. B.G.Bills, "A Spectral Domain Comparison of Two Recent Mars Gravity Models: GMM1 and Mars50c," Pre-print, Geodynamics Branch, NASA Goddard Space Flight Center, Greenbelt, Maryland.

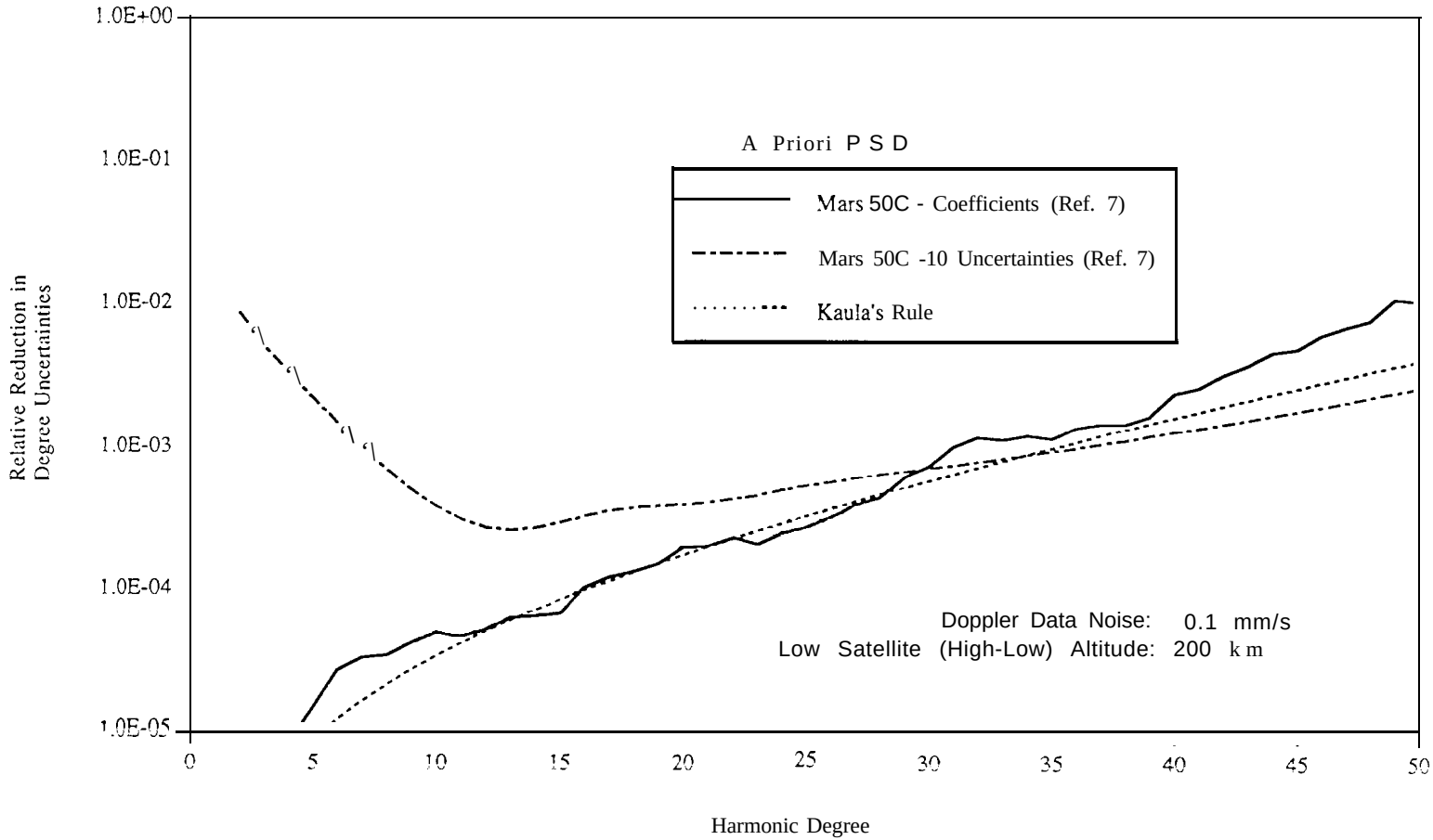

Figure 1

High-Low STS Doppler Data Performance Evaluation with Different A Priori PSD for Mars Gravity Field

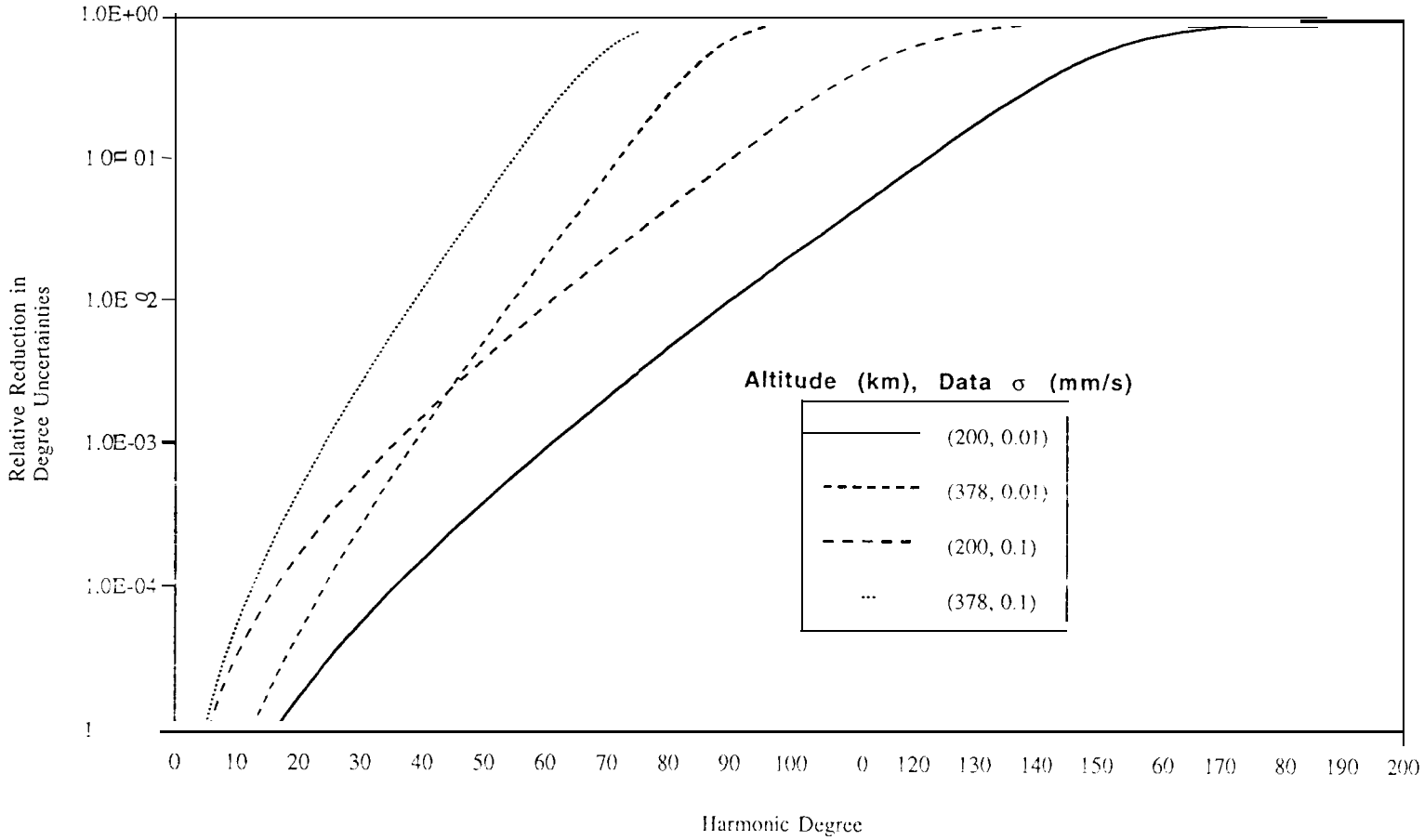

Figure 2
Sensitivity Results igh-Low STS Data

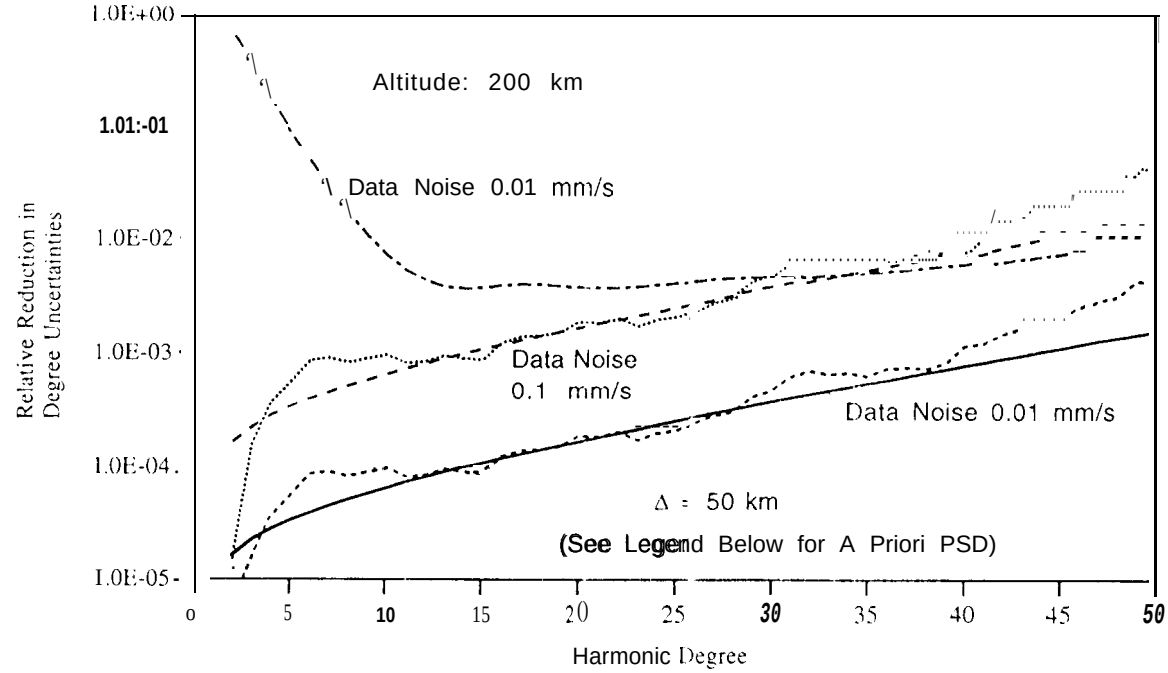

Figure 3a (Altitude -200 km)

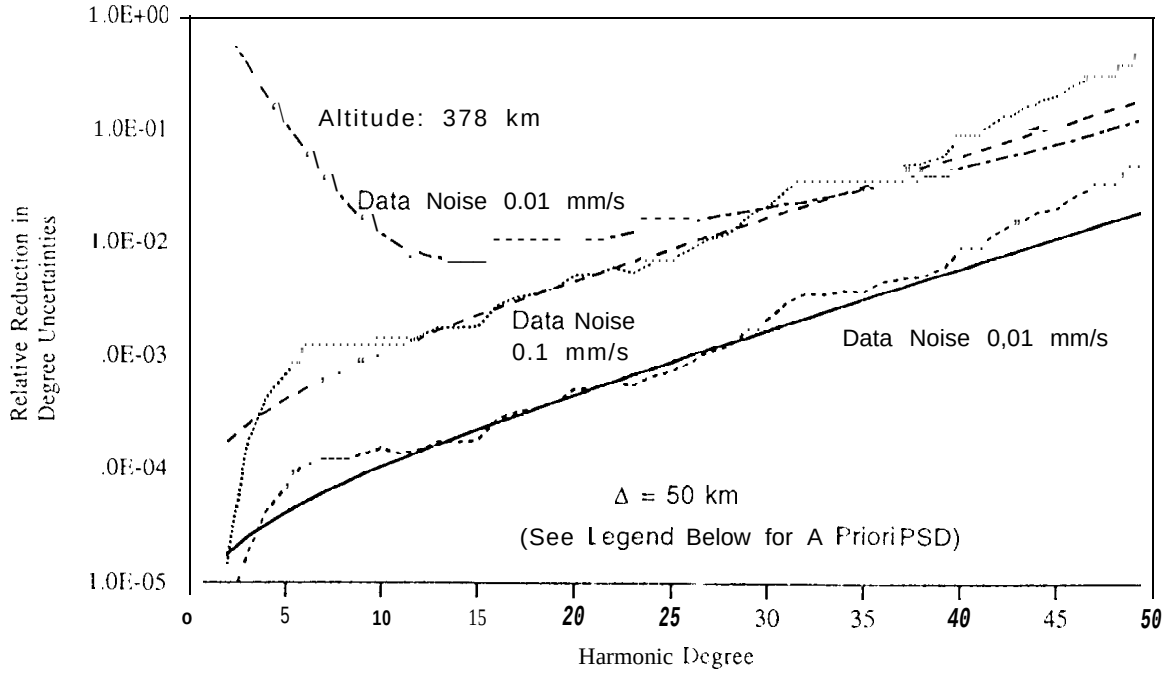

Figure 3b (Altitude - 378 km)

Figure 3
Low-Low STS Doppler Data Performance Evaluation with Different A Priori PSD for Mars Gravity Field and Data

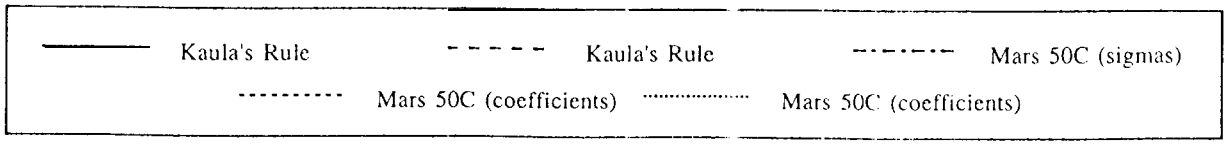

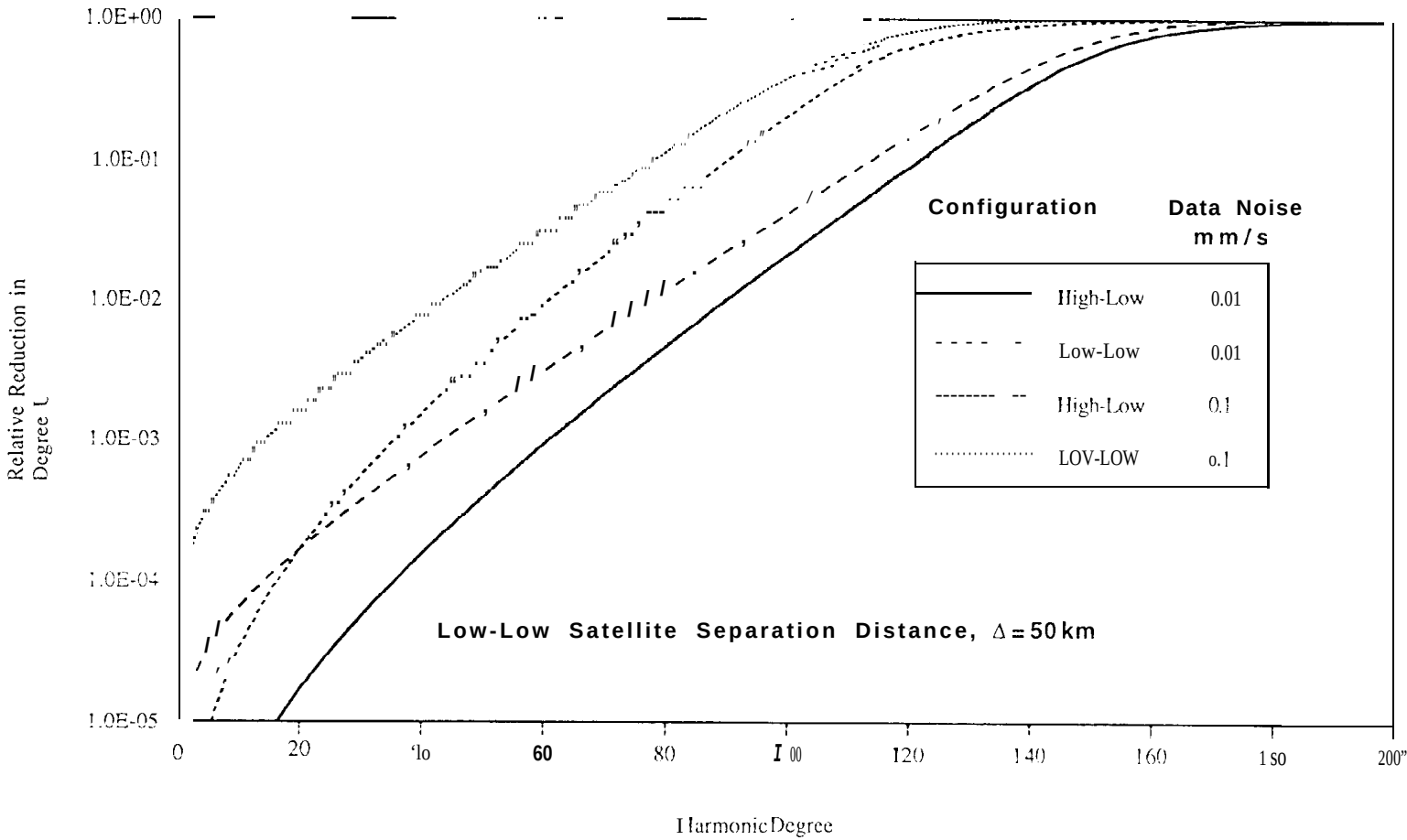

Figure 4
Performance Comparison of High-Low and Low-Low Satellite Configurations at different Data Noise Levels for (he Evaluation of Mars Gravity Field

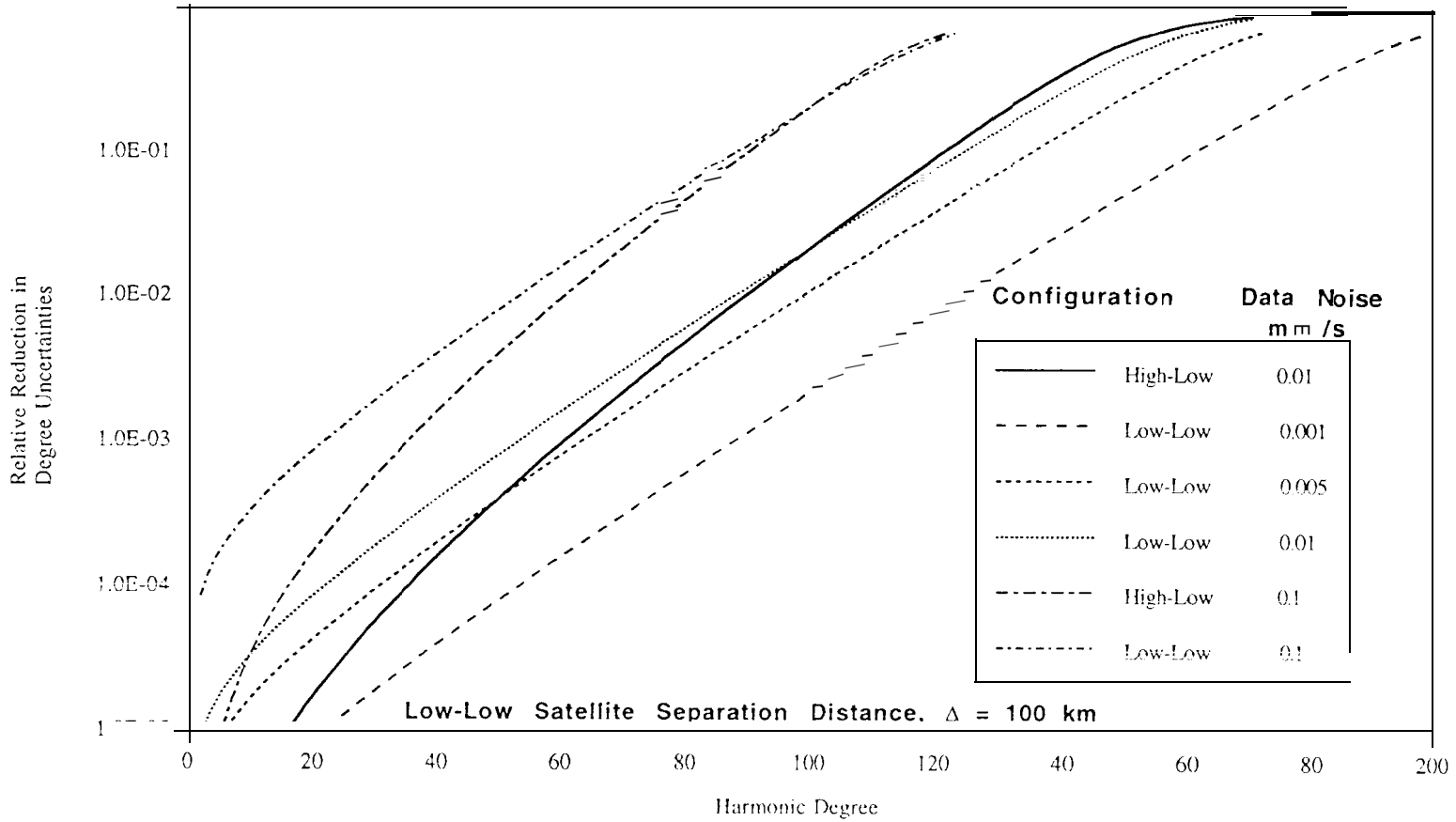

Figure 5
Performance Comparison of High-Low and Low-Low Satellite Configurations
at Different Data Noise Levels for the Evaluation of Mars Gravity Field

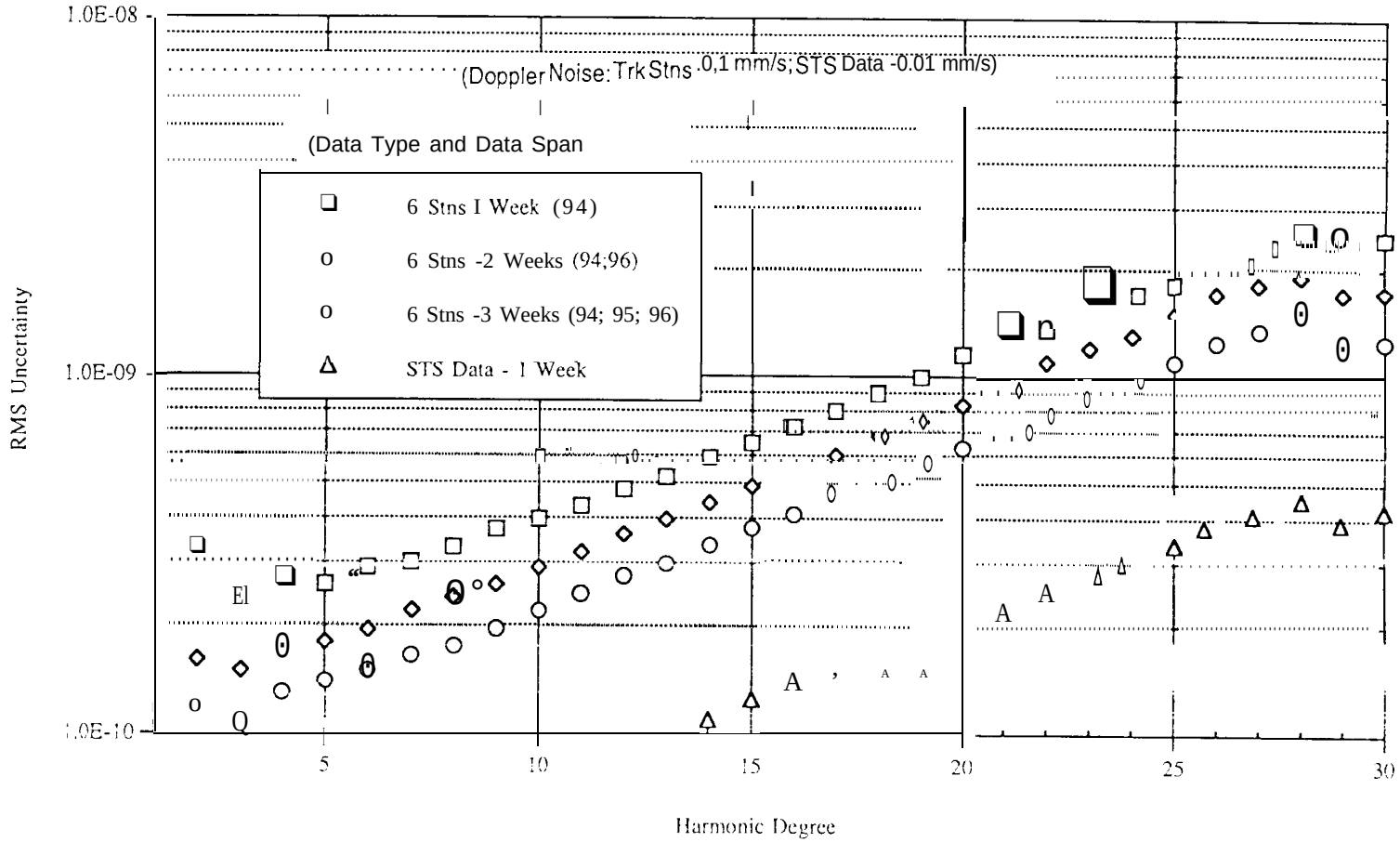

Figure 6
Effects of Data Type and Data Span on Spectral Uncertainties

Table 1. Average Surface Gravity Anomaly of Mars Gravity Field

(A Priori Values and A Posteriori Errors from STS Data.)

Averaging Kernel	1°	1°	$\frac{10}{2}$
	59.3 km	29.65 km	29.65 kill
A Priori Values of Average Surface Gravity Anomaly.			
	626.29	626.29	924.5
A Posteriori Errors in Average Surface Gravity Anomaly			
Low-Low Satellite Separation Distance, Δ	50 km	100 km	100 km
STS System / Data Noise mm/sec	(Gravity Anomalies in milligals)		
High-Low 0.01	11.44 (1.83)[a]	-	197.5 (21.36)
Low-Low 0.001	2.76 (0.44)	1.52 (0.24)	60.52 (6.55)
Low-Low 0.005	9.51 (1.52)	5.71 (0.91)	143.15 (15.48)
Low-Low 0.01	15.38 (2.46)	9.51 (1.52)	1S2.31 (19.72)
High-Low 0.1	42.43 (6.78)	--	328.4 (35.52)
Low-Low 0.1	61.54 (9.83)	41.95 (6.70)	328.22 (35.50)

[a] Entries inside parentheses are the ratios of *a posteriori* errors to a *priori* values expressed in percentages.